

Managing Micrometric Sources of Solvated Electrons: Application to the Local Functionalization of Fluorinated Self-Assembled Monolayers

Nadia Ktari,[†] Sandra Nunige,[†] Ammar Azioune,[‡] Matthieu Piel,[‡] Carole Connan,[§]
Frédéric Kanoufi,[†] and Catherine Combellas*,[†]

[†]*Physico-Chimie des Electrolytes, des Colloïdes et Sciences Analytiques, CNRS UMR 7195, ESPCI ParisTech, 10 rue Vauquelin, 75231 Paris Cedex 05, France, [‡]Laboratoire Compartimentation et Dynamique Cellulaire, CNRS UMR 144, Institut Curie, 26 rue d'Ulm, 75248 Paris Cedex 05, France, and [§]ITODYS, CNRS UMR 7086, Université Paris Diderot, 15 rue Jean de Baïf, 75013 Paris, France*

Received July 9, 2010. Revised Manuscript Received September 7, 2010

Microelectrodes allow micrometric sources of a solvated electron solution to be easily handled at room temperature. Such strongly reducing sources are the key for a new wet-chemical lithographic procedure. It is used to decorate the highly chemically inert surfaces of fluorosilane self-assembled monolayers grafted onto various inorganic surfaces with fluorescent moieties, or living cells.

Introduction

Controlling the surface chemistry of a material is a key issue in cell biology, miniaturized sensors or chips development, microfluidics, and so forth. For routine use, it requires the rapid and inexpensive prototyping of disposable devices, advantaging “soft-lithographic”¹ methods compared to standard clean-room lithographies.

Electrochemistry provides a versatile source of reactive reagents, which has been beneficial to monitor surface chemistry² or patterning³ in a clean and inexpensive way. However, the reactivity of the electrogenerated species, its E^0 , is usually restricted by its chemical stability or by the potential window of the electrolyte. The former drawback may be circumvented with submicrometric electrodes and/or homogeneous redox mediated processes. Macro-^{2b} or micrometric³ sources of highly oxidizing reagents, as reactive as plasma sources, have been proposed.

Here, we handle micrometric sources of solvated electron, e_{solv} , the most powerful reducer known.⁴ The high reactivity of e_{solv} sources is illustrated to activate the extremely stable C–F bond in fluorinated layers, which are well-known for their exceptional qualities such as hydrophobicity, solvophobicity, chemical inertness, thermal stability, low dielectric constant, and biocompatibility. These performances make fluorinated surfaces promising to design

microsystems such as microfluidic devices,⁵ superhydrophobic surfaces,⁶ or micropatterned surfaces for the manipulation and growth of cells.⁷ Perfluorinated silanes allow the easy formation of chemically inert layers of the most hydrophobic and oleophobic films,⁸ which should be good candidates for designing surfaces with patterned wettabilities. Indeed, a large wettability contrast is required in various microsystems such as those directed toward cells or particles manipulation and growth.^{7b,9,10}

However, owing to the extreme strength of the C–F bond, the patterning of perfluorinated surfaces is often delicate. Their low surface energy limits the adhesion of coating layers, which makes the use of photoresists difficult. Harsh activation procedures are often required, such as electron or ion beam techniques,¹¹ long time exposure to oxygen plasma,^{7b} or UV lithography that uses the photocatalytic activity of TiO_x .¹² Alternative

*Corresponding author. Tel. 33140794608; fax 33140794720; e-mail catherine.combellas@espci.fr.

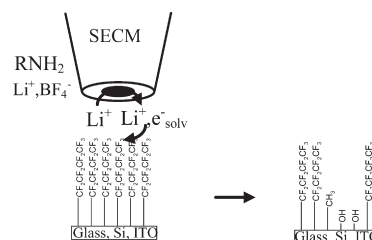
(1) Xia, Y.; Whitesides, G. M. *Angew. Chem., Int. Ed.* **1998**, *37*, 550.
(2) (a) Pinson, J.; Podvorica, F. *Chem. Soc. Rev.* **2005**, *34*, 429.
(b) McCreery, R. L. *Chem. Rev.* **2008**, *108*, 2646.
(3) (a) Mandler, D. In *Scanning Electrochemical Microscopy*; Bard, A. J., Mirkin, M. V., Eds.; Marcel Dekker: New York, 2001; p 593.
(b) Wittstock, G.; Burchardt, M.; Pust, S. E.; Shen, Y.; Zhao, C. *Angew. Chem., Int. Ed.* **2007**, *46*, 1584.
(4) Weyl, W. *Ann. Phys.* **1863**, *197*, 601.
(5) (a) Rolland, J. P.; Van Dam, R. M.; Schorzman, D. A.; Quake, S. R.; DeSimone, J. M. *J. Am. Chem. Soc.* **2004**, *126*, 2322.
(b) Gratton, S. E. A.; Williams, S. S.; Napier, M. E.; Pohlhaus, P. D.; Zhou, Z.; Wiles, K. B.; Maynor, B. W.; Shen, C.; Olafsen, T.; Samulski, E. T.; DeSimone, J. M. *Acc. Chem. Res.* **2008**, *41*, 1685.

(6) Hikita, M.; Tanaka, K.; Nakamura, T.; Kajiyama, T.; Takahara, A. *Langmuir* **2005**, *21*, 7299.
(7) (a) Krishnan, S.; Weinman, C. J.; Ober, C. K. *J. Mater. Chem.* **2008**, *18*, 3405. (b) Finlay, J. A.; Krishnan, S.; Callow, M. E.; Callow, J. A.; Dong, R.; Asgill, N.; Wong, K.; Kramer, E. J.; Ober, C. K. *Langmuir* **2008**, *24*, 503. (c) Senaratne, W.; Andruzzi, L.; Ober, C. K. *Biomacromolecules* **2005**, *6*, 2427.
(8) Wasserman, S. R.; Tao, Y.-T.; Whitesides, G. M. *Langmuir* **1989**, *5*, 1074.
(9) Kumar, A.; Biebuyck, H. A.; Whitesides, G. M. *Langmuir* **1994**, *10*, 1498.
(10) (a) Stenger, D. A.; Georger, J. H.; Dulcey, C. S.; Hickman, I. J.; Rudolph, A. S.; Nielsen, T. B.; McCort, S. M.; Calvert, J. M. *J. Am. Chem. Soc.* **1992**, *114*, 8435. (b) Spargo, B. J.; Testoff, M. A.; Nielsen, T. B.; Stenger, D. A.; Hickman, J. J.; Rudolph, A. S. *Proc. Natl. Acad. Sci. U.S.A.* **1994**, *91*, 11070. (c) Acaturk, T. O.; Peel, M. M.; Petrosko, P.; LaFramboise, W.; Johnson, P. C.; DiMilla, P. A. *J. Biomed. Mater. Res.* **1999**, *44*, 355. (d) Franco, M.; Nealey, P. F.; Campbell, S.; Teixeira, A. I.; Murphy, C. J. *J. Biomed. Mater. Res.* **2000**, *52*, 261.
(11) Luscombe, C. K.; Li, H. W.; Huck, W. T. S.; Holmes, Q. B. *Langmuir* **2003**, *19*, 5273.
(12) (a) Zhang, H.; Lee, Y. Y.; Leck, K. J.; Kim, N. Y.; Ying, J. Y. *Langmuir* **2007**, *23*, 4728. (b) Zhang, X.; Kono, H.; Liu, Z.; Nishimoto, S.; Tryk, S. A.; Murakami, T.; Sakai, H.; Abe, M.; Fujishima, A. *Chem. Commun.* **2007**, 4949.

patterning strategies were also proposed using either the local plasma growth of a perfluorinated layer onto Si¹³ or the local deposition of a fluorinated surface using specific hydrophobic interactions between fluorinated phases.¹⁴ These techniques are often difficult to transpose to every fluorinated material or to scale up. Organic chemistry or electrochemistry proposes alternative strategies to activate the C–F bond.¹⁵ Indeed, as confirmed theoretically,¹⁶ perfluoroalkyl chains are sensitive to reducers, in solution¹⁷ or in the gas phase.¹⁸

On the basis of our expertise in the electrochemical activation of fluorinated molecules^{17d,19} and polymers,²⁰ we propose using highly reductive species available to the electrochemist as, for example, the solvated electron, e_{solv} , which is stable for more than several minutes in few solvents such as liquid ammonia, amines, and tetrahydrofuran. The confinement of the electrogenerated etchant is achieved owing to a scanning probe technique. Scanning electrochemical microscopy (SECM)³ has been successfully used to decorate surfaces with different chemical functionalities or biological entities. This is achieved either by the local desorption,²¹ etching,²² or functionalization²³ of self-assembled monolayers (SAMs), the local denaturation of thin protein layers,²⁴ or the local electrografting of thin organic layers on electrodes.²⁵ The use of nanometer size electrodes or probes (such as in STM or

Scheme 1. Local Reduction of a Fluorinated SAM by e_{solv} in Ethylenediamine



conductive AFM) has ensured the electrochemical nanopatterning of SAMs.^{21a,26}

First, we study from wetting and spectroscopic analyses the reactivity of e_{solv} in liquid NH₃ on different SAM covered surfaces as compared to standard oxidizing treatments (Fenton, piranha). Then, a microelectrode is used to generate, at room temperature, a stable micrometric source of e_{solv} in dry ethylenediamine (Scheme 1), and it is scanned at a micrometer distance above a fluorinated SAM covered surface. The action of this electrogenerated reagent on the fluorinated SAM is demonstrated from the local surface analysis of the patterned surfaces. Fluorescent entities, gold nanoparticles, and living cells are finally selectively immobilized onto the patterned fluorinated SAMs.

In this way, solvated electrons, chemically inert fluorinated silane SAMs immobilized on different inorganic surfaces,⁸ and scanning electrochemical microscopy (SECM) are combined to design functional surfaces devoted to the immobilization of micro- to nanometric objects at a desired location on the inert fluorinated substrate.

Experimental Section

Superhydrophobic Glass. The superhydrophobic glass (SHG) was provided by Saint-Gobain Recherche group (France). A glass surface is decorated with a random array of glass nanopillars (100 nm height, 300 nm diameter, < 1 μm average inter-pillar distance) by a plasma etching process. The superhydrophobicity was conferred by subsequent silanization with a 1H,1H,2H,2H-perfluorodecyl-silane.

Substrates Preparation. Substrates were $\sim 1 \times 1 \text{ cm}^2$ Si (from 2 in. wafers, ACS, France) and glass surfaces (from 1.1 mm thick microscope slides). ITO was provided by Saint-Gobain Recherche (Aubervilliers, France).

Glass and silicon substrates were cleaned with freshly prepared piranha solution (70:30 v/v, concentrated H₂SO₄/aqueous H₂O₂ (35%)) at 150 °C for 30 min. ITO was cleaned in alkaline piranha solution (1:1 v/v, H₂O₂ (30%)/NH₄OH (25%)) at 70 °C for 1 h. *Caution: these piranha solutions may explode in contact with organic solution and must be carefully handled.* The substrates were then rinsed with pure water (Millipore, resistivity $\geq 18.2 \text{ M}\Omega \text{ cm}$), cleaned by ultrasonication in water for 1 min, and dried under nitrogen.

The fluorosilane SAM surfaces (designated as G-CF, Si-CF, ITO-CF) were obtained by silanization in the gas phase by placing the substrates in a sealed cell in the presence of an open flask of 1H,1H,2H,2H-perfluorodecyltrichlorosilane (CF₃(CF₂)₇(CH₂)₂SiCl₃, 97%), heated at 110 °C for 15 h. G-CF and Si-CF could also be obtained from silanization in a 0.5 vol % CCl₄ solution of the silane; G-Oct was prepared from triethoxyoctylsilane solution as preconized in ref 8.

- (13) Ayón, A. A.; Zhang, X.; Khanna, R. A. *Sens. Actuators, A* **2001**, *91*, 381.
- (14) Tae, G.; Lammertink, R. G. H.; Kornfield, J. A.; Hubbell, J. A. *Adv. Mater.* **2003**, *15*, 66.
- (15) Amii, H.; Uneyama, K. *Chem. Rev.* **2009**, *109*, 2119.
- (16) Paul, A.; Wannere, C. S.; Kasalova, V.; Schleyer, P. V. R.; Schaefer, H. F., III. *J. Am. Chem. Soc.* **2005**, *127*, 15457.
- (17) (a) Kavan, L.; Dousek, F. P. *J. Fluorine Chem.* **1988**, *41*, 383. (b) Pud, A. A.; Shapoval, G. S.; Kukhar, V. P.; Mikulina, O. E.; Gervits, L. L. *Electrochim. Acta* **1995**, *40*, 1157. (c) Marsella, J. A.; Gilcinski, A. G.; Coughlin, A. M.; Pez, G. P. *J. Org. Chem.* **1992**, *57*, 2856. (d) Combellas, C.; Kanoufi, F.; Thiébaud, A. *J. Phys. Chem. B* **2003**, *107*, 10894.
- (18) (a) Spyrou, S. M.; Sauers, I.; Christoprou, L. G. *J. Chem. Phys.* **1983**, *78*, 7200. (b) Ishii, I.; McLaren, R.; Hitchcock, A. P.; Jordan, K. D.; Choi, Y.; Robin, M. B. *Can. J. Chem.* **1988**, *66*, 2104.
- (19) Andrieux, C. P.; Combellas, C.; Kanoufi, F.; Savéant, J.-M.; Thiébaud, A. *J. Am. Chem. Soc.* **1997**, *119*, 9527.
- (20) (a) Boittiaux, V.; Boucetta, F.; Combellas, C.; Kanoufi, F.; Thiébaud, A.; Delamar, M.; Shanahan, M. E. *R. Polym. J.* **1999**, *40*, 2011 and references therein. (b) Combellas, C.; Kanoufi, F.; Nunige, S. *Chem. Mater.* **2007**, *19*, 3830 and references therein.
- (21) (a) Pust, S. E.; Szunerits, S.; Boukherroub, R.; Wittstock, G. *Nanotechnology* **2009**, *20*, 075302. (b) Wilhelm, T.; Wittstock, G. *Angew. Chem., Int. Ed.* **2003**, *42*, 2248. (c) Wittstock, G.; Schuhmann, W. *Anal. Chem.* **1997**, *69*, 5059.
- (22) (a) Zhao, C.; Witte, I.; Wittstock, G. *Angew. Chem., Int. Ed.* **2006**, *45*, 5469. (b) Shiku, H.; Takeda, T.; Yamada, H.; Matsue, T.; Uchida, I. *Anal. Chem.* **1995**, *67*, 312. (c) Matrab, T.; Hauquier, F.; Combellas, C.; Kanoufi, F. *ChemPhysChem* **2010**, *11*, 670. (d) Slim, C.; Tran, Y.; Chehimi, M. M.; Garraud, N.; Roger, J.-P.; Combellas, C.; Kanoufi, F. *Chem. Mater.* **2008**, *20*, 6677. (e) Zhao, C.; Zawisza, I.; Nullmeier, M.; Burchardt, M.; Trauble, M.; Witte, I.; Wittstock, G. *Langmuir* **2008**, *24*, 7605. (f) Zhao, C.; Burchardt, M.; Brinkhoff, T.; Beardsley, C.; Simon, M.; Wittstock, G. *Langmuir* **2010**, *26*, 8641.
- (23) Ku, S.-Y.; Wong, K.-T.; Bard, A. J. *J. Am. Chem. Soc.* **2008**, *130*, 2392.
- (24) (a) Kaji, H.; Tsukidate, K.; Matsue, T.; Nishizawa, M. *J. Am. Chem. Soc.* **2004**, *126*, 15026. (b) Kaji, H.; Kanada, M.; Oyamatsu, D.; Matsue, T.; Nishizawa, M. *Langmuir* **2004**, *20*, 16.
- (25) (a) Matrab, T.; Combellas, C.; Kanoufi, F. *Electrochem. Commun.* **2008**, *10*, 1230. (b) Coughlin, C.; Gohier, F.; Bélanger, D.; Mauzeroll, J. *Angew. Chem., Int. Ed.* **2009**, *48*, 4006.
- (26) Wouters, D.; Hoepfner, S.; Schubert, U. S. *Angew. Chem., Int. Ed.* **2009**, *48*, 1732.

Fenton solution was 1 M H_2O_2 /0.05 M H_2SO_4 aqueous solution containing 1 M FeCl_2 .

Electrolytic Solutions. Solvated electrons in liquid ammonia were obtained by dissolving 0.1 M of metallic sodium into 80 mL of liquid ammonia in an undivided cell²⁷ maintained at -38°C with a cryocooler. Nonaqueous electrolytic solutions were prepared from dimethylformamide (DMF), ethylene diamine, tri-*p*-tolylphosphine (TPP), tetrabutylammonium tetrafluoroborate, and lithium tetrafluoroborate of highest purification grade and of lowest water content (Sigma). Ethylene diamine was distilled under vacuum from potassium solutions. Stock solutions of LiBF_4 in ethylene diamine were prepared some minutes before use, and a minimum amount of water was maintained by addition of Li granular (Fluka). The low density of Li resulted in the formation of a supernatant layer of Li + solvated electrons (blue coloration) that prevents moisture penetration into the underlying bulk ethylenediamine solution. This stock solution is placed in the SECM protected environment (plastic glovebag), and for SECM patterning, aliquots were sampled from the underlying solution. DMF solutions were prepared some minutes before use without further purification. Aqueous solutions of potassium ferrocyanide (from Janssen Chimica) + potassium chloride (from Prolabo) were made up in high purity Millipore water (resistivity $> 18\text{ M}\Omega\text{ cm}$).

Electrochemical Cell. A three-electrode assembly made of a $25\text{ }\mu\text{m}$ Pt wire microelectrode, a $250\text{ }\mu\text{m}$ diameter Pt counter-electrode, and a $250\text{ }\mu\text{m}$ diameter Ag/AgCl reference electrode is used, as described previously.^{22c} The electrochemical cell is connected to a CH660C potentiostat (CH Instruments). Such a three-electrode assembly allows SECM experiments to be performed in droplets of solution ($< 10\text{ }\mu\text{L}$).

SECM Procedures. *a. Microelectrode Positioning.* The home-made SECM setup was described previously.²⁸ The microelectrode is held above the substrate in a $10\text{ }\mu\text{L}$ drop of a solution containing a redox probe (either 3 mM $\text{Fe}(\text{CN})_6^{4-}$ in water + 0.1 M KCl or 0.1 M tri-*p*-tolylphosphine, TPP, in DMF + 0.1 M NBu_4BF_4). The microelectrode is biased at a potential such that the redox probe is consumed under mass-transfer control ($E > 0.5\text{ V}$ vs Ag/AgCl for $\text{Fe}(\text{CN})_6^{4-}$ or $E = -3\text{ V}$ vs Ag/AgCl for TPP). When a steady current is attained, the microelectrode is approached along the z direction at $1\text{ }\mu\text{m/s}$ toward the substrate while the current is recorded. The substrate behaves as an insulator and hinders the diffusion of the redox probe to the microelectrode; as a result, the current decreases as the tip-substrate distance decreases. This approach curve is fitted with the theoretical approach curve for an insulating substrate and allows the microelectrode to be placed at a given tip-substrate distance. The same strategy is used to settle the substrate plane parallel to the x,y displacement of the microelectrode.

b. Substrate Patterning. The appropriate handling of micro-metric sources of highly reducing reagents requires water and oxygen free environments. As proposed earlier,²⁸ the SECM was operated under a controlled atmosphere, and the whole device was kept under argon in a polyethylene bag (glovebag, Aldrich) during the experiment. The humidity in the plastic bag was maintained as low as possible, $\text{RH} < 0.2$ with molecular sieves; this was checked by a hair hygrometer. When the surface is patterned with the e_{solv} reagent, an aqueous $\text{Fe}(\text{CN})_6^{4-}$ solution is used for the tip positioning; it is then withdrawn with cotton

wipe, and the region contacted with the solution is rinsed with water droplets and dried with N_2 . Then, $100\text{ }\mu\text{L}$ of a 0.1 M LiBF_4 solution of ethylene diamine is poured onto the substrate. The microelectrode is biased at the solvent discharge potential of -3.5 V (Ag/AgCl), and the tip is moved along the x or y direction at speed v for the patterning.

When the surface is patterned with the TPP anion radical in DMF, the aqueous solution is used to adjust the substrate planarity. Then, the aqueous solution is withdrawn, the substrate cleaned and dried, and the DMF solution is added so that the tip positioning and substrate patterning are performed with TPP as the redox probe. Once patterned, the surfaces are cleaned in copious amounts of acetone and water under ultrasonic activation.

XPS Analysis. XPS spectra were recorded using a Thermo VG Scientific ESCALAB 250 system fitted with a microfocused, monochromatic Al $\text{K}\alpha$ X-ray source (1486.68 eV) and a magnetic lens that increases the electron acceptance angle and hence the sensitivity. An X-ray beam of $320\text{ }\mu\text{m}$ size was used at voltage of 15 kV and a power of 75 W for the image and for the line scans, respectively. The spectra were acquired in the constant analyzer energy mode, with a pass energy of 150 and 20 eV for the survey and the narrow regions, respectively. The images were recorded in the constant retard ratio (CRR) mode with a $\Delta E/E = 4$. The Advantage software (version 3.51) was used for data processing. Spectral calibration was determined by setting the aliphatic C-C/C-H C 1s peak at 285 eV. The C 1s image was recorded over an area of $375 \times 500\text{ }\mu\text{m}^2$ in the constant retard ratio; it is obtained at the peak of the CF_2 fragment (energy 291.6 eV) and the background subtracted by considering the output signal at 282 eV.

ToF-SIMS Analysis. ToF-SIMS analyses were carried out with an ION-TOF ToF-SIMS IV spectrometer. Surface analysis was performed in the static mode. A 0.8 pA Ga^+ ion beam was used that was rastered on a $350 \times 500\text{ }\mu\text{m}^2$ surface area. The ionic density that reaches the surface was $\sim 5 \times 10^{10}\text{ ions s}^{-1}\text{ cm}^{-2}$. Mass peaks resolution was $\sim 0.007\text{ amu}$. The images were obtained at the mass peak for different characteristic negative or positive ion fragments.

Water Condensation Figures. Condensation was performed in a plexiglass cell. The sample was positioned on an electrolytic copper block covered by a water layer that ensured a thermal contact. The sample cooling was carried out by a Peltier element contacting the copper block; the Peltier element itself was cooled by water. The temperature was controlled by a K type thermocouple. The cell was filled with nitrogen that was saturated with water owing to bubbling in ultrapure water (milli-Q grade from the laboratory). Experiments were observed with a stereo microscope (Olympus) and a digital camera. The images were analyzed by ImageJ software (Scion Corporation). The whole setup is represented in Figure SI-1 in Supporting Information.

Cells Culture. RPE-1 (Retinal Pigment Epithelial human) cells were cultured at 37°C in Dulbecco's modified Eagle's medium (DMEM-F12) supplemented with 10% of fetal calf serum (FCS), 2 mM glutamine, and antibiotics in a humidified atmosphere containing 50% CO_2 . Prior to adding cells, the patterned fluorinated glass substrates were incubated with pluronic F-127 (Sigma) at 0.2% in phosphate buffered saline (PBS) for 1 h and room temperature, before incubation with fibronectin. Cells were seeded on fibronectin micropatterned surfaces at $1.5 \times 10^4\text{ cells/cm}^2$. Floating cells were removed 20 min later by gentle flushing and extensive washing of the surface.²⁹

(27) Combellas, C.; Kanoufi, F.; Thiebault, A. *J. Electroanal. Chem.* **2001**, 499, 144.

(28) Combellas, C.; Ghilane, J.; Kanoufi, F.; Mazouzi, D. *J. Phys. Chem. B* **2004**, 108, 6391.

(29) Azioune, A.; Storch, M.; Bornens, M.; Thery, M.; Piel, M. *Lab Chip* **2009**, 9, 1640.

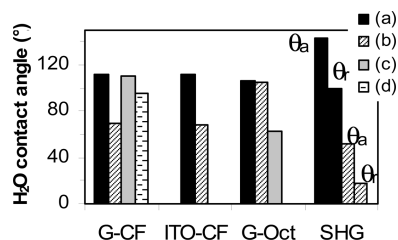


Figure 1. Water contact angles on different SAMs. Fluoroalkylsilane SAM on glass: G-CF, or ITO: ITO-CF, or nanostructured glass: SHG; octylsilane SAM on glass: G-Oct. (a) Pristine surfaces, action of (b) e_{solv} solution in NH_3 at $-38^\circ C$, (c) 15 min in Fenton solution, and (d) 10 min in piranha solution. θ_a , θ_r : advancing and receding angles, respectively.

Nikon Eclips TS100 microscope, equipped with DS camera control unit DS-L2, was used to record the phase contrast of living cells.

Results and Discussion

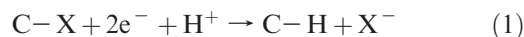
Etching of Hydrophobic or Superhydrophobic Surfaces.

Wetting and XPS Analysis. We compare the action of e_{solv} solution in liquid ammonia at $-38^\circ C$ and of classical oxidizing etchants on different hydrophobic or superhydrophobic surfaces. We inspect how these etchants change the surface wettability (Figure 1) of (i) glass surfaces covered either by SAMs of an octylsilane (G-Oct) or a 1*H*,1*H*,2*H*,2*H*-perfluorodecyl-silane (G-CF) or (ii) Si (Si-CF), ITO (ITO-CF), or a nanostructured glass (SHG) surface covered with the same perfluorinated SAM. The e_{solv} efficiently transforms, within less than 1 min, the perfluorinated glass (G-CF), Si (Si-CF, not shown, same as for G-CF), and ITO (ITO-CF) surfaces into more hydrophilic ones as the contact angle, θ , of a water sessile drop decreases from 112° to 70° after etching. It is even more spectacular for the superhydrophobic fluorinated glass (SHG of advancing contact angle, $\theta_a \sim 143^\circ$) as it is converted into an almost superhydrophilic substrate (receding contact angle, $\theta_r \sim 18^\circ$). Conversely, the e_{solv} has no action on the alkyl SAM (G-Oct), even after 10 min. This suggests that the e_{solv} reduces the fluorinated SAM and therefore that e_{solv} does not significantly decompose to reduce liquid ammonia to the strong alkali, NH_2^- .²⁷ Indeed, such strong alkali would have etched all silane SAMs independently of their chemical nature by dissociation of the Si–O–Si bonds. Therefore, the e_{solv} solution acts as a reducer, and the perfluoroalkyl SAMs are reducible.

If oxidizing reagents, such as HO^\bullet generated from Fenton solution, significantly etch the alkyl surface (for G-Oct, θ goes from 107° to 63°), they do not affect the perfluoroalkyl surfaces (even after 15 min). It confirms that alkylsilanes are sensitive to oxidants such as HO^\bullet ^{22b} (or Br_2 ^{22a}) and demonstrates that the perfluoroalkyl chains form a chemically inert blocking barrier to the transport of small molecules, such as HO^\bullet , as the ethyl chain of the fluorosilane adjacent to the surface was unetched. The fluorosilane layer resists to a lesser extent to harsher oxidizing conditions, as after a 10 min reaction in a piranha solution, the water contact angle decreases by $\sim 6^\circ$ (G-CF, 112° to 106°).

XPS analysis of the pristine and etched G-CF surfaces was carried out to evidence structural changes in the composition of the etched surfaces. Figure 2 presents the experimental and deconvoluted XPS spectra of the C 1s region of the glass–CF substrate before (Figure 2A) and after 3 min of immersion into a solvated electron solution (Figure 2B). The C 1s region was deconvoluted into hydrogenated (C–C, C–Si at a binding energy of 285 eV), oxygenated, and fluorinated carbons (290.6, 291.5, and 293.8 eV for CF_2 –C, CF_2 – CF_2 and CF_3 respectively). The proportion of the different peaks for unreduced G-CF is consistent with the chemical structure of the perfluorinated SAM immobilized onto SiO_2 . After reduction, both the higher energy peaks of fluorinated C 1s carbons (compare left parts in Figure 2A,B) and the F 1s/Si 2p ratio (not shown) are largely smaller, while the hydrogenated and oxygenated C 1s carbon and the O 1s/Si 2p ratio (not shown) are higher.

The defluorination and hydrogenation of the SAM are consistent with the general mechanism for electrochemical reductive C–X (X = halogen) bond cleavage according to



However, taking into account the conversion of C–F into C–H only does not explain the increase in surface wettability (compare θ for G-CF and G-Oct). Indeed, the complete hydrogenation of the perfluorinated chain cannot be invoked since a surface of low surface energy (with a water contact angle $> 100^\circ$ close to that of G-Oct) would be expected in disagreement with the observed value of $\theta_{G-CF-red} = 70^\circ$.

Such a low value for the contact angle rather results from the surface oxygenation (30%, estimated by XPS for oxygenated fragments). If the reductive process restored the original hydrophilic glass surface, the reduced surface would be a composite surface made of the restored hydrophilic original glass surface and of unreacted perfluorinated chains (or of hydrogenated chains with similar surface energy). The fractional coverage of the restored glass surface, Θ_1 of contact angle $\theta_{glass} \sim 10^\circ$, or of the unreacted (or hydrogenated) perfluorinated layer, $1 - \Theta_1$, of contact angle $\theta_{G-CF} = 112^\circ$, can be estimated from Cassie's equation³⁰ and the composite reduced surface contact angle, $\theta_{G-CF-red}$:

$$\cos \theta_{G-CF-red} = \Theta_1 \cos \theta_{glass} + (1 - \Theta_1) \cos \theta_{G-CF} \quad (2)$$

yielding $\Theta_1 = 0.5$. This value lower than the XPS estimate of 60–70% surface defluorination implies that the reduction and the oxygenation of the surface are not solely due to the restoration of the original glass surface. This is also confirmed from the presence of various carbonated fragments of lower binding energies (C–C, C–OH, C=O) in the C 1s region and because in the Si 2p region the peak relative to Si–O–C has not disappeared.

(30) Cassie, A. B. D. *Discuss. Faraday Soc.* **1952**, 75, 5041.

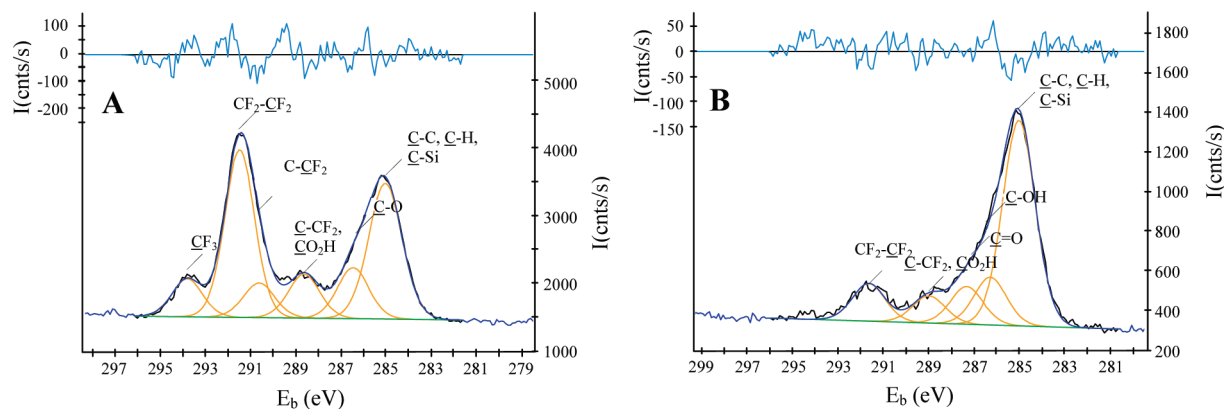
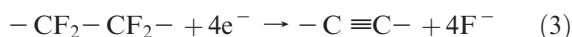


Figure 2. XPS spectra of the C 1s region of (A) a fluorinated glass, G-CF, and (B) a fluorinated glass reduced for 3 min by a solution of solvated electron in liquid ammonia (-38°C).

Finally, the increase of wettability rather results from a combination of partial glass restoration and formation of C–O fragments within the etched perfluoroalkyl chain since the reduction of perfluorinated substrates yields unsaturated sites reactive toward water and oxygen:¹⁷



Then, the post-treatment formation of C–O, by exposition to air and water of the reduced surface, is also consistent with a mechanism of reduction of the perfluoroalkyl chain.

Patterning of Fluorinated SAM Surfaces. Micro-XPS, Micro-ToF-SIMS, and Water Condensation Characterizations. The reductive etching process is transposed at a local scale for the patterning of fluorinated SAM surfaces (Scheme 1). A microelectrode of $12.5\text{ }\mu\text{m}$ radius is positioned according to SECM principle, at $2\text{--}4\text{ }\mu\text{m}$ from the SAM surface. The local micrometric source of solvated electrons is obtained, at room temperature, by reduction at a Pt microelectrode of 0.1 M LiBF_4 in dry ethylenediamine ($\text{H}_2\text{NCH}_2\text{CH}_2\text{NH}_2$), by polarizing the microelectrode at the decomposition potential of the electrolyte (i.e., -3.5 V (Ag/AgCl)); it ensures the generation at the microelectrode of e_{solv} with a cathodic current, $i < -100\text{ nA}$. Large cathodic potentials or currents are necessary to ensure a sufficient amount of e_{solv} owing to its low stability in the hygroscopic ethylenediamine. From the microelectrode steady-state current, the amount of e_{solv} generated at the microelectrode surface is about 20 mM . It is likely less important at the SAM surface owing to possible reaction with the solvent and/or traces of water/oxygen. In most classical organic solvents such as DMF, e_{solv} cannot be produced, but the electro-generated radical anion of tri(*p*-tolyl)-phosphine ($E^0 = -2.75\text{ V (SCE)}$)³¹ is the closest to electrolyte discharge reducer that we found to efficiently pattern the SAM.

The etching of the fluorinated SAM is a slow process as the microelectrode must fly over each substrate point for, at least, 1 s for the formation of visible pattern. This is

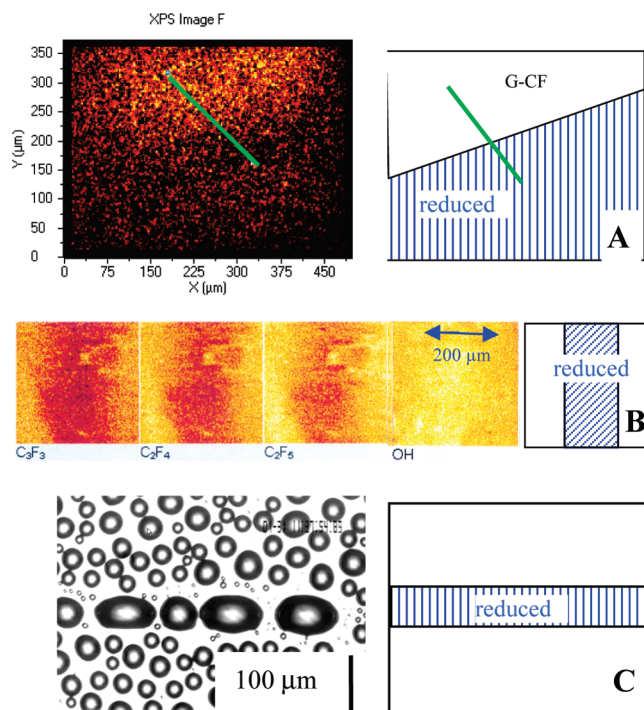


Figure 3. (A) Micro XPS images of the CF_2 contribution of a locally reduced perfluorinated glass. (B) Micro ToF-SIMS images of a locally reduced perfluorinated glass (from left to right: positive perfluorinated fragments, C_3F_3^+ , C_2F_4^+ , C_2F_5^+ , and OH^-). (C) Water condensation figure on a $75\text{ }\mu\text{m}$ wide stripe patterned on Si-CF.

supported from previous wettability investigation.³² This slowness of the etching is the limiting factor of the patterning speed, v , and the microelectrode should not travel faster than $v < 25\text{ }\mu\text{m/s}$. For comparison, the complete reduction of bromo-terminated SAMs is still efficient at much faster writing speeds. It is in agreement with the weakness of C–Br compared to C–F.^{22d} It confirms that perfluoroalkyl chains are highly stable and that even e_{solv} is not a sufficiently efficient reducer. However, fast and high throughput patterning (compared to standard lithographic techniques using masks and stamps) are obtained by using “stamp” electrodes.³³ It

(31) Fuchs, A.; Kanoufi, F.; Combellas, C.; Shanahan, M. E. R. *Colloids Surf., A* **2007**, *307*, 7.

(32) Combellas, C.; Fuchs, A.; Kanoufi, F.; Shanahan, M. E. R. In *Contact Angle, Wettability and Adhesion*; Mittal, K. L., Eds.; V.S.P.: Utrecht, 2006; Vol. 4, pp 43–59.

(33) (a) Combellas, C.; Fuchs, A.; Kanoufi, F. *Anal. Chem.* **2004**, *76*, 3612. (b) Deiss, F.; Combellas, C.; Fretigny, C.; Sojic, N.; Kanoufi, F. *Anal. Chem.* **2010**, *82*, 5169.

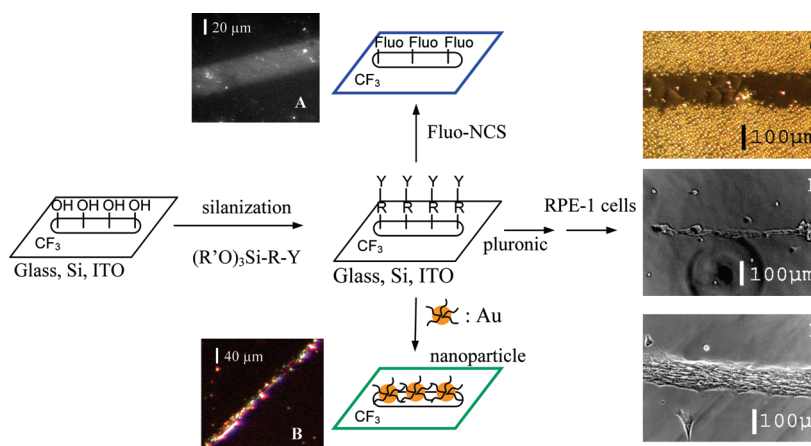


Figure 4. Selective post-functionalization of a locally reduced perfluorinated surface. Coupling of the patterned surface with (A) a fluorescent probe and (B) gold nanoparticles. Selective adhesion of living RPE-1 cells on the patterned surface (characterized by water condensation (C) after (D) few hours or (E) 3 days of immersion in the culture medium).

is particularly demonstrated by the imprint of lines when using band or wire as “stamp” electrodes. The use of micro-electrode arrays should be possible too; however, the array proposed previously for the patterning of Teflon^{33b} cannot be applied here since it used arrays made from thin gold layers which are expected to be readily dissolved under extremely reducing conditions and particularly in solvated electrons solutions.³⁴

The reductive patterning of fluorinated SAMs (G-CF) is characterized from micro-XPS and micro-ToF SIMS. Local XPS supports the mechanism observed on wholly reduced surfaces, with a loss of fluorine $\sim 70\%$ in the reduced region (Figure 3A). Defluorination is confirmed from ToF-SIMS images of perfluorinated ions abstracted from the patterned surface (Figure 3B, first three images for $C_3F_3^+$, $C_2F_4^+$, and $C_2F_5^+$). ToF-SIMS also shows that the reduced region is richer in OH^- (fourth image in Figure 3B) and CH^- (not shown) and poorer in C^+ fragments (not shown), in agreement with the hydroxylation, hydrogenation, and possible chain fragmentation, respectively.

According to this patterning procedure, a hydrophilic pattern is formed within a surrounding hydrophobic fluorinated SAM. It is evidenced from the preferred condensation of water vapor onto the patterns (Figure 3C). Breath figures evidence patterns of contrasted wettabilities;³⁵ they also allow surface contact angle, θ , estimate when the condensation process has reached a self-similar regime observed at long condensation time.³⁶ Typically, this regime was reached in Figure 3C after 300 s of condensation with a 100 mL/min flux of 19 °C N_2 over a patterned surface held at 11 °C. Then, the surface contact angle, θ , is correlated to the droplet surface coverage, ε^2 : the lower θ , the more the surface is covered by droplets, also, for $10^\circ < \theta < 90^\circ$:

$$\theta \sim \frac{(1 - \varepsilon^2) \times 90^\circ}{1 - 0.55} \quad (4)$$

(34) Teherani, T. H.; Peer, W. J.; Lagowski, J. J.; Bard, A. J. *J. Am. Chem. Soc.* **1978**, *100*, 7768.

(35) (a) López, G. P.; Biebuyck, H. A.; Frisbie, C. D.; Whitesides, G. M. *Science* **1993**, *260*, 647. (b) Kumar, A.; Biebuyck, H. A.; Whitesides, G. M. *Langmuir* **1994**, *10*, 1498.

A droplet surface occupation of 0.67 ± 0.02 in the pattern (Figure 3C) indicates a mean contact angle of $66 \pm 4^\circ$ within the pattern, in good agreement with the value observed on totally etched surfaces (Figure 1). Breath figures showed that 30 to 200 μm wide patterns are drawn, depending on the reducer and writing speed. The pattern width was assessed independently from the selective anchoring of a fluorescent tag (see below).

Patterns Post-Functionalization. Patterns derivatization was envisioned according to the spectroscopic analyses, which show that the reductive surface treatment (at the local or global levels) introduces $-OH$ groups onto the surface. The concentration of these $-OH$ groups was enhanced by post-treating the surface with Fenton or piranha solutions, which affect only the patterned region. Indeed, from breath figures, θ decreases to 50° within the pattern after 10 min in a Fenton bath. Then, the surface $-OH$ groups were engaged into silanization reactions to design hydrophobic perfluorinated surfaces patterned with chosen chemical functionalities.

By reaction with aminopropyltriethoxysilane (APTES), NH_2 functions were selectively introduced into the patterned region and further derivatized with fluorescein-isothiocyanate to bind fluorescein tags within the pattern (Figure 4A). The contact angle within the (unreduced) fluorinated surface is unchanged after the successive derivatization steps, confirming that the latter did not take place on the inert G-CF surface.

The pattern width obtained from fluorescence tagging is ~ 1 tip radius larger than the breath figures estimate. The two determination methods are in acceptable agreement but also show that the patterns have diffuse borders due to the diffusion of the e_{solv} during the etching. The dimension of patterns with diffuse chemical functionalities is difficult to estimate from breath figures as it is difficult to deconvolute properly from local wetting analysis the contribution of both the pattern width and its surface energy distribution.³²

Thiolates were also introduced by reaction of the patterned surfaces with 3-mercaptopropyl-trimethoxysilane

(36) Zhao, H.; Beysens, D. *Langmuir* **1995**, *11*, 627.

(MPTMS). As a result, gold nanoparticles were selectively assembled into the patterned region (Figure 4B) by dipping a patterned Si-CF surface into a gold colloid solution.³⁷

Finally, the patterned surfaces were used for cells culture. A surface reduced on a cm^2 region by dipping into an e_{solv} solution was incubated with RPE-1 cells. Cells adhered preferentially onto the reduced region and not onto the perfluorinated surface (Supporting Information, Figure SI-2). On micrometer scale patterns, the same procedure did not allow cell adhesion even after silanization of the surface with APTES. This was due to the adsorption of proteins, present in the cell culture medium and/or secreted by cells, onto perfluorinated regions.^{7b} To enhance selective cell adhesion, patterned surfaces were then incubated with a pluronic solution to prevent proteins adsorption on unreduced regions. Indeed, pluronic is known to adsorb preferentially onto hydrophobic surfaces and to prevent protein and cell adhesion. This simple surface treatment allowed to selectively assemble a single continuous line of RPE-1 cells on the patterns, as depicted in Figure 4D. For longer incubation times, the cell arrangement (Figure 4E) neatly reproduces the pattern observed by breath figures (Figure 4C).

(37) Doron, A.; Katz, E.; Willner, I. *Langmuir* **1995**, *11*, 1313.

Conclusion

Micrometric sources of the strongest reducer known, e_{solv} , are easily handled at room temperature. Combination of macro- and micro-spectroscopic and wetting analyses shows that the etching of fluorinated SAMs by e_{solv} results in surface defluorination and oxygenation. By standard post-silanization procedures, the patterned surfaces can be selectively decorated with fluorescent probes, gold particles, or living cells. This procedure is a promising alternative lithography of fluorinated silanes SAMs on different inorganic surfaces. Such lithographic strategy is easily transposable to the patterning of any fluorinated hydrophobic or superhydrophobic material surface.

Acknowledgment. Hervé Arribart and Arnaud Huignard (Saint-Gobain Recherche) are gratefully acknowledged for supplying of the hydrophobic glass. Janine Mauzeroll (UQAM, Canada) and Zsolt Lenkei (ESPCI, France) are acknowledged for helpful preliminary discussions on cell-adhesion assays. The “Agence Nationale de la Recherche” is acknowledged for its financial support via the ANR-06-BLAN-0368 project.

Supporting Information Available: Figures depicting the experimental setup for water condensation investigation and adhesion of living REP-1 cells onto a large reduced surface. This material is available free of charge via the Internet at <http://pubs.acs.org>.